



## INTERNATIONAL JOURNAL OF ENGINEERING SCIENCES & RESEARCH TECHNOLOGY

### Effect of Thermal Diffusion and Heat Absorption on an Unsteady MHD Flow Past a Flat Plate in Presence of Viscous Dissipation

**K.Anitha**

BVRIT Hyderabad College of engineering for women, Rajeev Gandhi Nagar, Hyderabad-90,  
India

[anithareddy1981@gmail.com](mailto:anithareddy1981@gmail.com)

#### Abstracts

The present work is devoted to the numerical study of the effect of Heat absorption and thermal diffusion on an unsteady magnetohydrodynamic(MHD) flow of a viscous incompressible and electrically conducting fluid past along a porous flat plate taking in to account Viscous dissipation. The governing equations and the associated boundary conditions for this analysis are made non dimensional forms using dimensionless variables. The governing equations are solved numerically by using Galerkin finite element method. The flow phenomenon has been characterized with the help of parameters such as Hartmann number, Grashof number and Modified Grashof number, Schmidt Number, Prandtl Number, Eckert number, Soret number and Heat absorption. The effect of all such parameters on the fluid velocity, temperature, concentration field, the skin – friction, the rate of heat and mass transfer have been examined and presented graphically and discussed qualitatively.

**Keywords:** Finite element method, Heat absorption, MHD, Thermal diffusion.

#### Nomenclature

$C'$	Dimensionless concentration	$\mu$	Viscosity, Ns/m <sup>2</sup>
$C_w$	Concentration near the plate	$\mu_e$	Magnetic permeability, Henry/meter
$C_\infty$	Concentration in the fluid far away from the plate	$C_p$	Specific heat at constant Pressure, J/kg-K
$\theta$	Dimensionless Temperature	$\rho$	Density, kg/m <sup>3</sup>
$T$	Temperature of the fluid	$\omega_e$	Electron frequency, radian/sec
$T_w$	Temperature of the plate	$D$	Chemical molecular diffusivity
$T_\infty$	Temperature of the fluid far away from the plate	$\tau_e$	Electron collision time in Sec
$u'$	Velocity component in $x'$ – direction	$e$	Electron charge, coulombs
$w'$	Velocity component in $z'$ - direction	$M$	Hartmann number
$x'$	Spatial co – ordinate along the plate	$n_e$	Number density of the electron
$\nu$	Kinematics viscosity, m <sup>2</sup> /s	Pr	Prandtl number
$y'$	Spatial co – ordinate normal to the plate	$P_e$	Electron Pressure, N/ m <sup>2</sup>
$\alpha$	Thermal Diffusivity	Sc	Schmidt Number
$k_e$	Mean absorption coefficient	$g$	Acceleration due to Gravity, 9.81 m/s <sup>2</sup>
$V_o$	Velocity vector, m/s	Gr	Grashof Number
$k$	Thermal conductivity, W/mK	Gc	Modified Grashof Number
$\sigma$	Electrical conductivity, mho/m	Sr	Soret Number
		$\beta$	Volumetric co – efficient of thermal Expansion, K <sup>-1</sup>
		Ec	Eckert number
		$\beta^*$	Co – efficient of volume expansion with Specie concentration

$Q$  Heat absorption coefficient

## Introduction

The problems of mixed convective MHD flows are of prime importance in a number of industrial applications in Geo-physical and Astro-Physical situations. The problem of convective MHD flows has wide range of publications in emerging fields viz granular insulation, geothermal systems in heating and cooling chambers, fossil fuel, combustion, energy process, solar energy and space vehicle re – entry. Some examples in living organisms are fluid transport mechanism among which the blood flow in circulatory system, with flow in airways. A classical example is in nuclear power station where the separation of uranium  $U_{235}$  from  $U_{238}$  by gases diffusion takes place.

Brinkman [1] was the first to estimate the viscous force imparted by a flowing fluid in a dense swarm of particles. Hassmoto [2] discussed the boundary layer growth on a flat plate with suction or injection. The two dimensional steady state flow of an incompressible viscous fluid with parallel rigid with porous wall with the flow being given by uniform suction or injection was studied by Berman [3]. Subsequently, the work of Berman was examined by Sellars [4] for high section Reynolds's number. Mori [5] consider the flow between two vertical plates which are electrically non-conducting under the assumption that the wall temperature varies linearly in the direction of the flow and the existence of the heat source in the vertical channel.

Later, Macey [6] examined the flow in the renal tubules as viscous flow through a circular tube of uniform cross section and permeable boundary by prescribing their radial velocity at the wall as exponentially decreasing function of axial distance. England and Emery [7] have studied the thermal radiation effects of an optically thin gray gas bounded by a stationary vertical plate, while Soundlegkar and Thakar [8] have examined the radiative free convective flow of an optically thin gray gas past a semi infinite vertical plate. Mansuutti et al. [9] had examined the steady flows of a non-Newtonian fluid past a porous plate with a suction or injection.

Sattar[10] reported the free convection and mass transfer flow through a porous medium past an infinite vertical porous plate with time dependent temperature and concentration. The radiation effects on flow past an impulsively started infinite isothermal vertical plate has been examined by Das et al. [11]. Chowdhary and Dass [12] investigated the magnetohydrodynamic boundary layer flow of a non

Newtonian fluid past a flat plate. Later, Das et al. [13] obtained numerically approximations for the mass transfer effects on unsteady flow past an accelerated vertical porous plate.

The objective of this paper is to study the thermal diffusion on unsteady MHD flow past along a porous flat plate in presence of heat absorption. The governing boundary layer equations along with the initial and boundary conditions are first cast into a dimensionless form and the resulting system of equations are then solved by finite element technique. The behaviour of the velocity, temperature, concentration, skin-friction, Nusselt number and Sherwood number has been discussed for variations in the governing thermo physical and hydro dynamical parameters.

## Mathematical formulation

Consider the unsteady mixed convection mass transfer flow of a viscous incompressible electrically conducting fluid past an accelerating vertical infinite porous flat plate in the presence of transversal magnetic

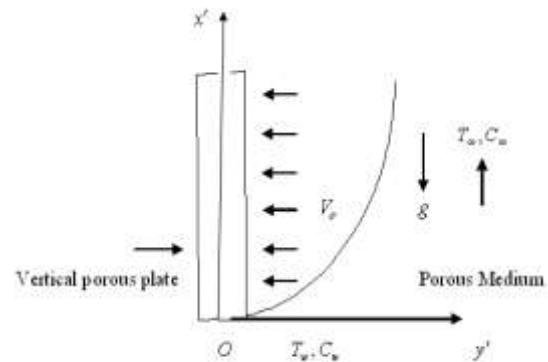


Figure 1. Physical sketch and geometry of the problem

field  $B_o$ . The  $x'$  – axis is directed upward along the plate and  $y'$  – axis normal to the plate with  $u$ , being the velocity component along the  $x'$  – axis. It is assumed that the plate is accelerating with a velocity  $u = U_o$  in its own plane for  $t \geq 0$ . The magnetohydrodynamic unsteady mixed convective boundary layer equations under the Boussinesq's approximations are:

$$\frac{\partial v}{\partial y'} = 0 \Rightarrow v = -V_0 \tag{1}$$

$$\frac{\partial u'}{\partial t'} + v \frac{\partial u'}{\partial y'} = v \frac{\partial^2 u'}{\partial y'^2} + g\beta(T - T_\infty) + g\beta^*(C - C_\infty) - \frac{\sigma B_o^2}{\rho} u' \tag{2}$$

$$\frac{\partial T}{\partial t'} + v \frac{\partial T}{\partial y'} = \frac{k}{\rho c_p} \frac{\partial^2 T}{\partial y'^2} + \frac{v}{c_p} \left( \frac{\partial u'}{\partial y'} \right)^2 - \frac{Q_o}{\rho c_p} (T - T_\infty) \tag{3}$$

$$\frac{\partial C}{\partial t'} + v \frac{\partial C}{\partial y'} = D \frac{\partial^2 C}{\partial y'^2} + \frac{D_m k_T}{T_m} \frac{\partial^2 T}{\partial y'^2} \tag{4}$$

The initial and boundary conditions of the problem are:

$$\left. \begin{aligned} t' \leq 0: & \quad u' = 0, \quad T = T_\infty, \quad C' = C_\infty \quad \text{for all } y' \\ t' > 0: & \quad \left\{ \begin{aligned} u' = 0, \quad T = T_w, \quad C' = C_w & \quad \text{at } y' = 0 \\ u' = 0, \quad T = T_\infty, \quad C' = C_\infty & \quad \text{as } y' \rightarrow \infty \end{aligned} \right. \end{aligned} \right\} \tag{5}$$

Introducing the following non - dimensional quantities:

$$\left. \begin{aligned} y^* &= \frac{V_o y'}{v}, u^* = \frac{u'}{V_o}, t^* = \frac{t' V_o^2}{v}, \theta^* = \frac{T - T_\infty}{T_w - T_\infty}, \\ C^* &= \frac{C - C_\infty}{C_w - C_\infty}, Gr = \frac{g\beta v (T_w - T_\infty)}{V_o^3}, Gc = \frac{g\beta^* v (C_w - C_\infty)}{V_o^3}, \\ Pr &= \frac{v \rho c_p}{k}, Sc = \frac{v}{D}, Q = \frac{v Q_o}{\rho c_p V_o^2}, Ec = \frac{V_o^2}{c_p (T_w - T_\infty)}, \\ Sr &= \frac{D_m k_T (T_w - T_\infty)}{v T_m (C_w - C_\infty)}, M = \frac{\sigma B_o^2 v}{\rho V_o^2} \end{aligned} \right\} \tag{6}$$

Equations (2) to (4) were reduce to the form and the stars (\*) ignored for readability

$$\frac{\partial u}{\partial t} - \frac{\partial u}{\partial y} = \frac{\partial^2 u}{\partial y^2} + (Gr)\theta + (Gc)C - Mu \tag{7}$$

$$\frac{\partial \theta}{\partial t} - \frac{\partial \theta}{\partial y} = \frac{1}{Pr} \frac{\partial^2 \theta}{\partial y^2} + Ec \left( \frac{\partial u}{\partial y} \right)^2 - Q\theta \tag{8}$$

$$\frac{\partial C}{\partial t} - \frac{\partial C}{\partial y} = \frac{1}{Sc} \frac{\partial^2 C}{\partial y^2} + Sr \left( \frac{\partial^2 \theta}{\partial y^2} \right) \tag{9}$$

The initial and boundary conditions (5) in the non - dimensional form are:

$$\left. \begin{aligned} t \leq 0: & \quad u = 0, \quad \theta = 0, C = 0 \quad \text{for all } y \\ t > 0: & \quad \left\{ \begin{aligned} u = 0, \quad \theta = 1, C = 1 & \quad \text{at } y = 0 \\ u = 0, \quad \theta = 0, C = 0 & \quad \text{as } y \rightarrow \infty \end{aligned} \right. \end{aligned} \right\} \tag{10}$$

**Method of solution**

By applying Galerkin finite element method for equation (7) over the element (e), (y<sub>j</sub> ≤ y ≤ y<sub>k</sub>) is:

$$\int_{y_j}^{y_k} N^{(e)T} \left[ \frac{\partial^2 u^{(e)}}{\partial y^2} - \frac{\partial u^{(e)}}{\partial t} + \frac{\partial u^{(e)}}{\partial y} - Mu^{(e)} + P \right] dy = 0 \tag{11}$$

Where P = (Gr)θ + (Gc)C ;

Integrating the first term in equation (11) by parts one obtains

$$N^{(e)T} \left\{ \frac{\partial u^{(e)}}{\partial y} \right\}_{y_j}^{y_k} - \int_{y_j}^{y_k} \left[ \frac{\partial N^{(e)T}}{\partial y} \frac{\partial u^{(e)}}{\partial y} + N^{(e)T} \left( \frac{\partial u^{(e)}}{\partial t} - \frac{\partial u^{(e)}}{\partial y} + Mu^{(e)} - P \right) \right] dy = 0 \tag{12}$$

Neglecting the first term in equation (12), one gets:

$$\int_{y_j}^{y_k} \left[ \frac{\partial N^{(e)T}}{\partial y} \frac{\partial u^{(e)}}{\partial y} + N^{(e)T} \left( \frac{\partial u^{(e)}}{\partial t} - \frac{\partial u^{(e)}}{\partial y} + Mu^{(e)} - P \right) \right] dy = 0$$

Let u<sup>(e)</sup> = N<sup>(e)</sup>ϕ<sup>(e)</sup> be the linear piecewise approximation solution over the element (e) (y<sub>j</sub> ≤ y ≤ y<sub>k</sub>)

where N<sup>(e)</sup> = [N<sub>j</sub> N<sub>k</sub>], ϕ<sup>(e)</sup> = [u<sub>j</sub> u<sub>k</sub>]<sup>T</sup> and

N<sub>j</sub> =  $\frac{y_k - y}{y_k - y_j}$ , N<sub>k</sub> =  $\frac{y - y_j}{y_k - y_j}$  are the basis functions. One obtains:

$$\int_{y_j}^{y_k} \left\{ \begin{bmatrix} N'_j & N'_j & N'_j & N'_k \\ N'_j & N'_k & N'_k & N'_k \end{bmatrix} \begin{bmatrix} u_j \\ u_k \end{bmatrix} \right\} dy + \int_{y_j}^{y_k} \left\{ \begin{bmatrix} N_j & N_j & N_j & N_k \\ N_j & N_k & N_k & N_k \end{bmatrix} \begin{bmatrix} \dot{u}_j \\ \dot{u}_k \end{bmatrix} \right\} dy$$

$$- \int_{y_j}^{y_k} \left\{ \begin{bmatrix} N_j & N_j & N_j & N_k \\ N'_j & N'_k & N'_k & N'_k \end{bmatrix} \begin{bmatrix} u_j \\ u_k \end{bmatrix} \right\} dy + M \int_{y_j}^{y_k} \left\{ \begin{bmatrix} N_j & N_j & N_j & N_k \\ N_j & N_k & N_k & N_k \end{bmatrix} \begin{bmatrix} u_j \\ u_k \end{bmatrix} \right\} dy$$

$$= P \int_{y_j}^{y_k} \begin{bmatrix} N_j \\ N_k \end{bmatrix} dy$$

Simplifying we get

$$\frac{1}{l^{(e)^2}} \begin{bmatrix} 1 & -1 \\ -1 & 1 \end{bmatrix} \begin{bmatrix} u_j \\ u_k \end{bmatrix} + \frac{1}{6} \begin{bmatrix} 2 & 1 \\ 1 & 2 \end{bmatrix} \begin{bmatrix} \dot{u}_j \\ \dot{u}_k \end{bmatrix} - \frac{1}{2l^{(e)}} \begin{bmatrix} -1 & 1 \\ -1 & 1 \end{bmatrix} \begin{bmatrix} u_j \\ u_k \end{bmatrix} +$$

$$\frac{M}{6} \begin{bmatrix} 2 & 1 \\ 1 & 2 \end{bmatrix} \begin{bmatrix} u_j \\ u_k \end{bmatrix} = \frac{P}{2} \begin{bmatrix} 1 \\ 1 \end{bmatrix}$$

Where prime and dot denotes differentiation w.r.t  $y$  and time  $t$  respectively. Assembling the element equations for two consecutive elements  $y_{i-1} \leq y \leq y_i$  and  $y_i \leq y \leq y_{i+1}$  following is obtained:

$$\frac{1}{l^{(e)^2}} \begin{bmatrix} 1 & -1 & 0 \\ -1 & 2 & -1 \\ 0 & -1 & 1 \end{bmatrix} \begin{bmatrix} u_{i-1} \\ u_i \\ u_{i+1} \end{bmatrix} + \frac{1}{6} \begin{bmatrix} 2 & 1 & 0 \\ 1 & 4 & 1 \\ 0 & 1 & 2 \end{bmatrix} \begin{bmatrix} \dot{u}_{i-1} \\ \dot{u}_i \\ \dot{u}_{i+1} \end{bmatrix} -$$

$$\frac{1}{2l^{(e)}} \begin{bmatrix} -1 & 1 & 0 \\ -1 & 0 & 1 \\ 0 & -1 & 1 \end{bmatrix} \begin{bmatrix} u_{i-1} \\ u_i \\ u_{i+1} \end{bmatrix} + \frac{M}{6} \begin{bmatrix} 2 & 1 & 0 \\ 1 & 4 & 1 \\ 0 & 1 & 2 \end{bmatrix} \begin{bmatrix} u_{i-1} \\ u_i \\ u_{i+1} \end{bmatrix} = \frac{P}{2} \begin{bmatrix} 1 \\ 2 \\ 1 \end{bmatrix} \quad (13)$$

Now put row corresponding to the node  $i$  to zero, from equation (13) the difference schemes with  $l^{(e)} = h$  is:

$$\frac{1}{h^2} [-u_{i-1} + 2u_i - u_{i+1}] + \frac{1}{6} [\dot{u}_{i-1} + 4\dot{u}_i + \dot{u}_{i+1}] - \frac{1}{2h} [-u_{i-1} + u_{i+1}] +$$

$$\frac{M}{6} [u_{i-1} + 4u_i + u_{i+1}] = P \quad (14)$$

Applying the trapezoidal rule, following system of equations in Crank – Nicholson method are obtained:

$$A_1 u_{i-1}^{n+1} + A_2 u_i^{n+1} + A_3 u_{i+1}^{n+1} = A_4 u_{i-1}^n + A_5 u_i^n + A_6 u_{i+1}^n + P^* \quad (15)$$

Now from equations (8) and (9), following equations are obtained:

$$B_1 \theta_{i-1}^{n+1} + B_2 \theta_i^{n+1} + B_3 \theta_{i+1}^{n+1} = B_4 \theta_{i-1}^n + B_5 \theta_i^n + B_6 \theta_{i+1}^n + Q^{**}$$

(16)

$$D_1 C_{i-1}^{n+1} + D_2 C_i^{n+1} + D_3 C_{i+1}^{n+1} = D_4 C_{i-1}^n + D_5 C_i^n + D_6 C_{i+1}^n + R^* \quad (17)$$

Where

$$A_1 = 2 + Mk + 3rh - 6r, A_2 = 8 + 4Mk + 12r,$$

$$A_3 = 2 + Mk - 3rh - 6r, A_4 = 2 - Mk - 3rh + 6r,$$

$$A_5 = 8 - 4Mk - 12r, A_6 = 2 - Mk + 3rh + 6r,$$

$$B_1 = 2(\text{Pr}) + 3rh(\text{Pr}) - 6r, B_2 = 8(\text{Pr}) + 12r,$$

$$B_3 = 2(\text{Pr}) - 3rh(\text{Pr}) - 6r,$$

$$B_4 = 2(\text{Pr}) - 3rh(\text{Pr}) + 6r, B_5 = 8(\text{Pr}) - 12r,$$

$$B_6 = 2(\text{Pr}) + 3rh(\text{Pr}) + 6r,$$

$$D_1 = 2(\text{Sc}) + 3rh(\text{Sc}) - 6r, D_2 = 8(\text{Sc}) + 12r,$$

$$D_3 = 2(\text{Sc}) - 3rh(\text{Sc}) - 6r,$$

$$D_4 = 2(\text{Sc}) - 3rh(\text{Sc}) + 6r, D_5 = 8(\text{Sc}) - 12r,$$

$$D_6 = 2(\text{Sc}) + 3rh(\text{Sc}) + 6r,$$

$$P^* = 12Phk = 12hk(\text{Gr})\theta_i^j + 12hk(\text{Gc})C_i^j,$$

$$Q^{**} = 12kQ^* = 12k(\text{Pr})Ec \left( \frac{\partial u}{\partial y} \right)^2,$$

$$R^* = 12kR = 12k(\text{Sc})(\text{Sr}) \left( \frac{\partial^2 \theta}{\partial y^2} \right);$$

Here  $r = \frac{k}{h^2}$  and  $h, k$  are mesh sizes along  $y$  – direction and time – direction respectively. Index  $i$  refers to space and  $j$  refers to the time. In the equations (15), (16) and (17), taking  $i = 1(1)n$  and using boundary conditions (10), then the following system of equations are obtained:

$$A_i X_i = B_i, \quad i = 1(1)3 \quad (18)$$

where  $A_i$ 's are matrices of order  $n$  and  $X_i, B_i$ 's are column matrices having  $n$  – components. The solutions of above system of equations are obtained by using Thomas algorithm for velocity, temperature and concentration. Also, numerical solutions for these equations are obtained by  $C$  – programme. In order to prove the convergence and stability of Galerkin finite element method, the same  $C$  – programme was run with smaller values of  $h$  and  $k$  and no significant change was observed in the values of  $u, \theta$  and  $C$ . Hence the Galerkin finite element method is stable and convergent.

## Results and discussions

We solve the similarity equations (7), (8) and (9) numerically subject to the boundary conditions given by (10). In this study, we investigate the influence of the effects of material parameters such as Hartmann number ( $M$ ), Grashof Number for heat and mass transfer ( $Gr, Gc$ ), Schmidt Number ( $Sc$ ), Prandtl Number ( $Pr$ ), Eckert number ( $Ec$ ), Soret number ( $Sr$ ) and Heat absorption ( $Q$ ) separately in order to clearly observe their respective effects on the velocity, temperature and concentration profiles of the flow. And also skin – friction coefficients ( $\tau$ ), Rate of heat and mass transfer coefficients in terms of Nusselt number ( $Nu$ ) and Sherwood number ( $Sh$ ) respectively have been observed through graphically. During the course of numerical calculations of the velocity ( $u$ ), temperature ( $\theta$ ) and concentration ( $C$ ). For the physical significance, the numerical discussions in the problem and at  $t = 1.0$ , stable values for velocity, temperature and concentration fields are obtained. To examine the effect of parameters related to the problem on the velocity field and skin – friction numerical computations are carried out at  $Pr = 0.71$ . To find solution of this problem, we have placed an infinite vertical plate in a finite length in the flow. Hence, we solve the entire problem in a finite boundary. However, in the graphs, the  $y$  values vary from 0 to 4, and the velocity, temperature, and concentration tend to zero as  $y$  tend to 4. This is true for any value of  $y$ . Thus, we have considered finite length.

The temperature and the species concentration are coupled to the velocity via Grashof number  $Gr$  and Modified Grashof number  $Gc$  as seen in equation (7). For various values of Grashof number and Modified Grashof number, the velocity profiles  $u$  are plotted in figures (2) and (3). As expected, it is observed that there is a rise in the velocity due to the enhancement of thermal buoyancy force, as  $Gr$  increases, also it is noticed that the velocity increases with increasing values of the Modified Grashof number  $Gc$ .

Figure (4) and (10) depicts the effect of Prandtl number on velocity profiles and the Temperature profiles in presence of foreign species such as Mercury ( $Pr = 0.025$ ), Air ( $Pr = 0.71$ ) and Water ( $Pr = 7.00$ ). It is observed that an increase in the Prandtl number leads to decrease in the temperature field. We observe that from figure (5) the velocity decreases with increasing of Prandtl number.

The nature of velocity profiles in presence of foreign species such as Hydrogen ( $Sc = 0.22$ ), Helium ( $Sc = 0.30$ ), Water vapour ( $Sc = 0.60$ ) and Oxygen ( $Sc = 0.66$ ) are shown in figure (5). The flow field suffers a decrease in velocity at all points in presence of heavier diffusing species. From figure (6) it is clear that the velocity of the fluid decreases with the increase of the magnetic field number values i.e Hartmann number ( $M$ ). Because the presence of a magnetic field in an electrically conducting fluid introduces a force called the Lorentz force, which acts against the flow if the magnetic field is applied in the normal direction.

The influence of the viscous dissipation parameter i.e., the Eckert number ( $Ec$ ) on the velocity and temperature are shown in figures (7) and (11) respectively. Greater viscous dissipative heat causes a rise in the temperature as well as the velocity. This behavior is evident from figures (7) and (11). Figures (8) and (12) illustrate the influence of heat absorption coefficient ( $Q$ ) on the velocity and temperature at  $t = 1.0$  respectively. Physically speaking, the presence of heat absorption (thermal sink) effects has the tendency to reduce the fluid temperature. This causes the thermal buoyancy effects to decrease resulting in a net reduction in the fluid velocity. These behaviors are clearly obvious from figures (8) and (12). The variations of velocity distribution with  $y$  for different values of the Soret number ( $Sr$ ) are shown in figure (9). It can be clearly seen that the velocity distribution in the boundary layer increases with the Soret number. It is interesting note that the effect of Soret number on velocity field is little significant. This is because either a decrease in concentration difference or an increase in temperature difference leads to an increase in the value of the Soret parameter ( $Sr$ ).

The effects of Schmidt number ( $Sc$ ) and Soret number ( $Sr$ ) on the concentration field are presented in figures (13) and (14). Figure (13) shows the concentration field due to variation in Schmidt number ( $Sc$ ) for the gasses Hydrogen, Helium, Water – vapour, Oxygen and Ammonia. It is observed that concentration field is steadily for Hydrogen and falls rapidly for Oxygen and Ammonia in comparison to Water – vapour. Thus Hydrogen can be used for maintaining effective concentration field and Water – vapour can be used for maintaining normal concentration field. In figure (14), it is observed that an increase in the Soret number ( $Sr$ ) leads to increase in the concentration field.

**Graphs:**

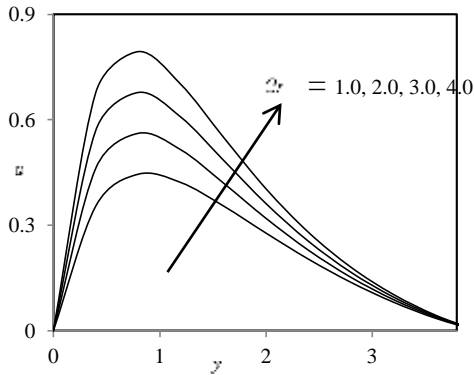


**Figure 2.** Effect of  $Gr$  on velocity profiles when  $G_c = 1.0$ ,  $Sc = 0.22$ ,  $M = 1.0$ ,  $Pr = 0.71$ ,  $Sr = 1.0$ ,  $Ec = 0.001$  and  $Q = 1.0$ .

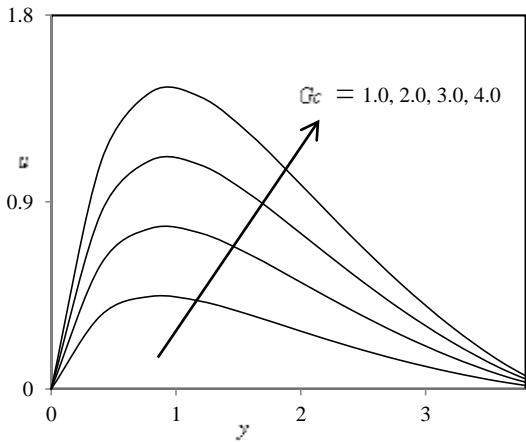


**Figure 3.** Effect of  $G_c$  on velocity profiles when  $Gr = 1.0$ ,  $Sc = 0.22$ ,  $M = 1.0$ ,  $Pr = 0.71$ ,  $Sr = 1.0$ ,  $Ec = 0.001$  and  $Q = 1.0$ .

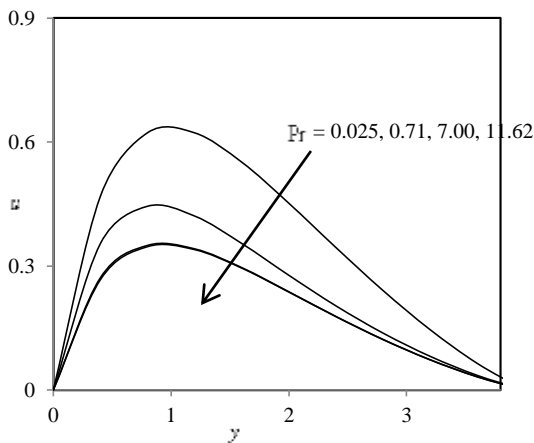


**Figure 4.** Effect of  $Pr$  on velocity profiles when  $Gr = 1.0$ ,  $G_c = 1.0$ ,  $Sc = 0.22$ ,  $M = 1.0$ ,  $Sr = 1.0$ ,  $Ec = 0.001$  and  $Q = 1.0$ .

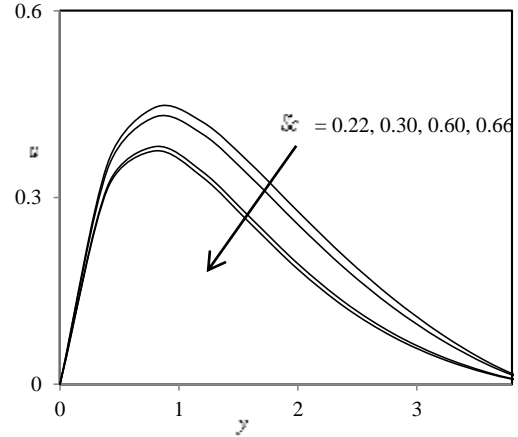


**Figure 5.** Effect of  $Sc$  on velocity profiles when  $Gr = 1.0$ ,  $G_c = 1.0$ ,  $M = 1.0$ ,  $Pr = 0.71$ ,  $Sr = 1.0$ ,  $Ec = 0.001$  and  $Q = 1.0$ .

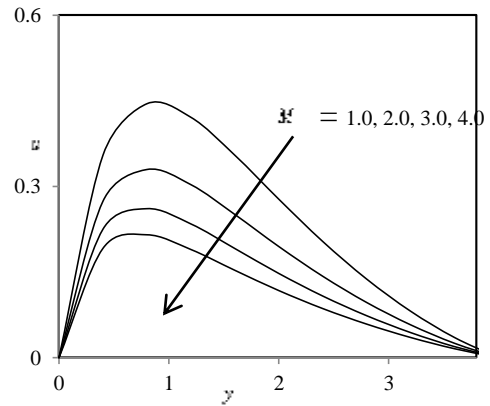


**Figure 6.** Effect of  $M$  on velocity profiles when  $Gr = 1.0$ ,  $G_c = 1.0$ ,  $Sc = 0.22$ ,  $Pr = 0.71$ ,  $Sr = 1.0$ ,  $Ec = 0.001$  and  $Q = 1.0$ .

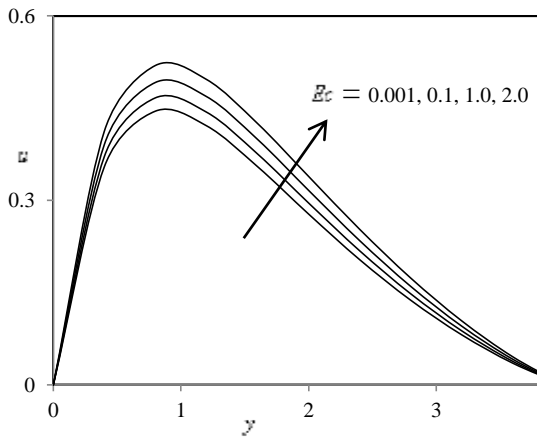


Figure 7. Effect of  $E_c$  on velocity profiles when  $Gr = 1.0$ ,  $G_c = 1.0$ ,  $Sc = 0.22$ ,  $M = 1.0$ ,  $Pr = 0.71$ ,  $Sr = 1.0$  and  $Q = 1.0$ .

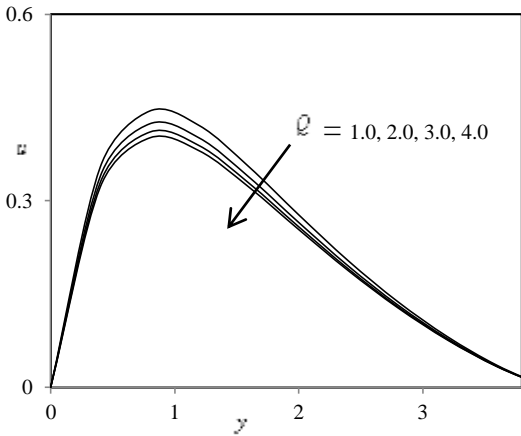


Figure 8. Effect of  $Q$  on velocity profiles when  $Gr = 1.0$ ,  $G_c = 1.0$ ,  $Sc = 0.22$ ,  $M = 1.0$ ,  $Pr = 0.71$ ,  $Sr = 1.0$  and  $E_c = 0.001$ .

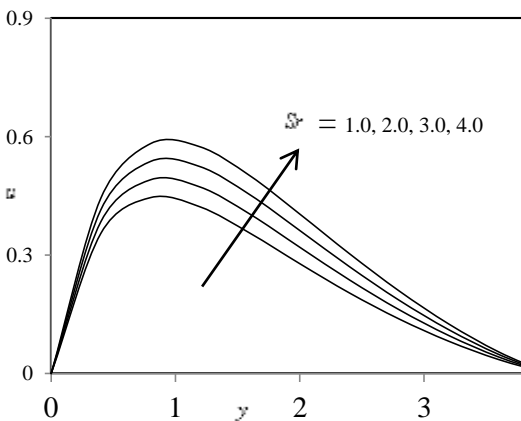


Figure 9. Effect of  $Sr$  on velocity profiles when  $Gr = 1.0$ ,  $G_c = 1.0$ ,  $Sc = 0.22$ ,  $M = 1.0$ ,  $Pr = 0.71$ ,  $E_c = 0.001$  and  $Q = 1.0$ .

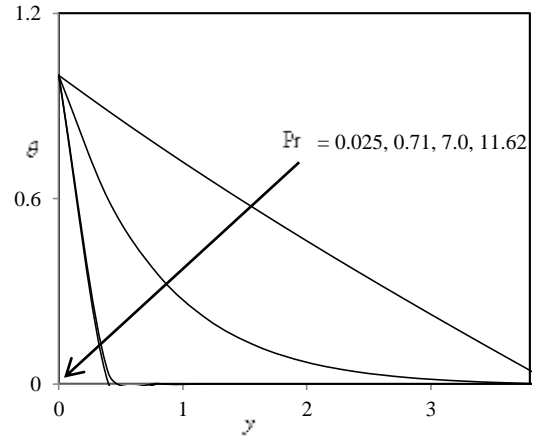


Figure 10. Effect of  $Pr$  on temperature profiles when  $Gr = 1.0$ ,  $G_c = 1.0$ ,  $Sc = 0.22$ ,  $M = 1.0$ ,  $Sr = 1.0$ ,  $E_c = 0.001$  and  $Q = 1.0$ .

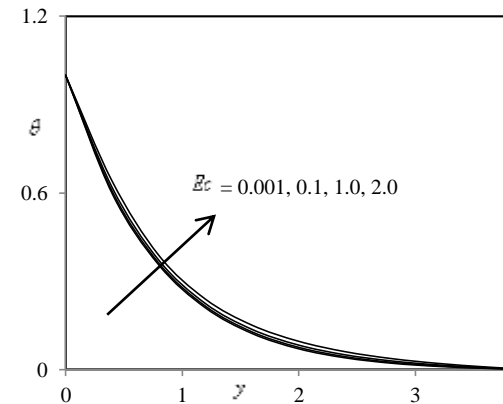


Figure 11. Effect of  $E_c$  on temperature profiles when  $Gr = 1.0$ ,  $G_c = 1.0$ ,  $Sc = 0.22$ ,  $M = 1.0$ ,  $Pr = 0.71$ ,  $Sr = 1.0$  and  $Q = 1.0$ .

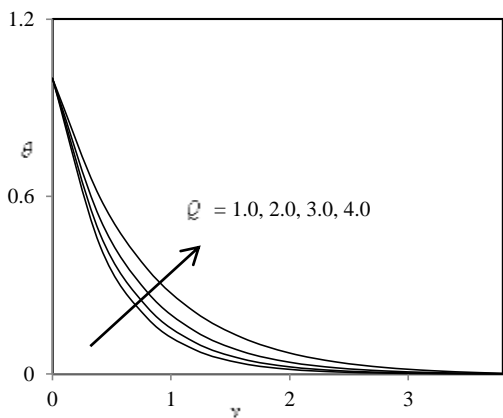


Figure 12. Effect of  $Q$  on temperature profiles when  $Gr = 1.0$ ,  $Gc = 1.0$ ,  $Sc = 0.22$ ,  $M = 1.0$ ,  $Pr = 0.71$ ,  $Sr = 1.0$  and  $Ec = 0.001$ .

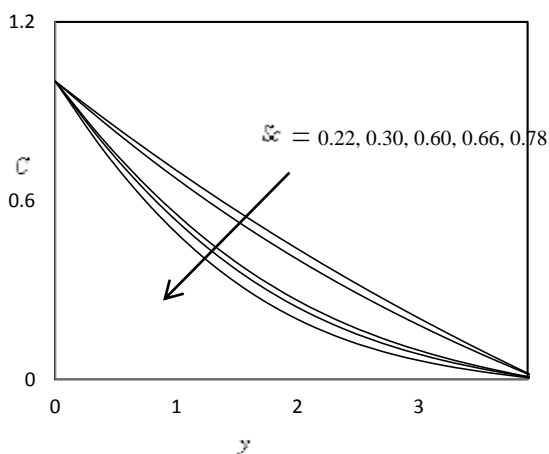


Figure 13. Effect of  $Sc$  on concentration profiles when  $Gr = 1$ ,  $Gc = 1.0$ ,  $M = 1.0$ ,  $Pr = 0.71$ ,  $Sr = 1.0$ ,  $Ec = 0.001$  and  $Q = 1.0$ .

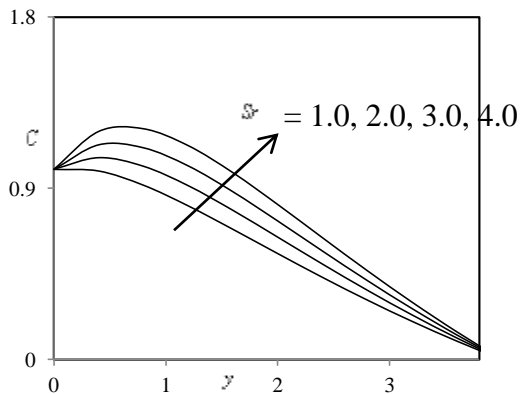


Figure 14. Effect of  $Sr$  on concentration profiles when  $Gr = 1.0$ ,  $Gc = 1.0$ ,  $Sc = 0.22$ ,  $M = 1.0$ ,  $Pr = 0.71$ ,  $Ec = 0.001$  and  $Q = 1.0$ .

Skin – friction, Rate of heat and mass transfer :

The expression for skin – friction coefficient ( $\tau$ ) at the plate is  $\tau = \left(\frac{\partial u}{\partial y}\right)_{y=0}$  (19)

Heat transfer coefficient ( $Nu$ ) at the plate is  $Nu = -\left(\frac{\partial \theta}{\partial y}\right)_{y=0}$  (20)

Mass transfer coefficient ( $Sh$ ) at the plate is  $Sh = -\left(\frac{\partial C}{\partial y}\right)_{y=0}$  (21)

The results for skin – friction ( $\tau$ ) due to velocity under the effect of Hartmann number ( $M$ ), Grashof number  $Gr$  and Modified Grashof number  $Gc$ , Schmidt Number ( $Sc$ ), Prandtl Number ( $Pr$ ), Eckert number ( $Ec$ ), Soret number ( $Sr$ ) and Heat absorption ( $Q$ ) are presented in the table 1.

Table 1. Skin–friction coefficient( $\tau$ ) due to velocity profiles.

$Gr$	$Gc$	$Pr$	$Sc$	$M$	$Q$	$Ec$	$Sr$	$\tau$
1.0	1.0	0.71	0.22	1.0	1.0	0.001	1.0	4.4580
2.0	1.0	0.71	0.22	1.0	1.0	0.001	1.0	5.5809
1.0	2.0	0.71	0.22	1.0	1.0	0.001	1.0	7.7933
1.0	1.0	7.0	0.22	1.0	1.0	0.001	1.0	3.5288
1.0	1.0	0.71	0.30	1.0	1.0	0.001	1.0	4.2949
1.0	1.0	0.71	0.22	2.0	1.0	0.001	1.0	3.2787
1.0	1.0	0.71	0.22	1.0	2.0	0.001	1.0	4.2491
1.0	1.0	0.71	0.22	1.0	1.0	0.100	1.0	4.4623
1.0	1.0	0.71	0.22	1.0	1.0	0.001	2.0	4.9380

From this table we observe that the skin – friction coefficient increases with the increasing values of Grashof number  $Gr$  and Modified Grashof number  $Gc$ , Eckert number ( $Ec$ ) and Soret number ( $Sr$ ) and decreases with the increasing values of Schmidt Number ( $Sc$ ), Prandtl Number ( $Pr$ ) and Heat absorption ( $Q$ ).



**Table 2. Nusselt number ( $Nu$ ) due to temperature profiles**

Pr	$Ec$	$Q$	$Nu$
0.71	0.001	1.0	3.1186
7.0	0.001	1.0	2.1056
0.71	0.10	1.0	3.1338
0.71	0.001	2.0	2.3587

The profiles for Nusselt number ( $Nu$ ) due to temperature profile under the effect of Prandtl Number ( $Pr$ ), Eckert number ( $Ec$ ) and Heat absorption ( $Q$ ) are presented in the table 2. We see from this table the Nusselt number ( $Nu$ ) due to temperature profile decreases under the effect Prandtl Number ( $Pr$ ) and Heat absorption ( $Q$ ) and increases under the effect of Eckert number ( $Ec$ ).

**Table 3. Sherwood number ( $Sh$ ) due to concentration profiles**

$Sc$	$Sr$	$Sh$
0.22	1.0	7.8990
0.30	1.0	7.8312
0.22	2.0	8.9169

The profiles for Sherwood number ( $Sh$ ) due to concentration profile under the effect of Schmidt number ( $Sc$ ) and Soret number ( $Sr$ ) are presented in the table 3. From this table we observed that Sherwood number ( $Sh$ ) due to concentration profile rises under the effect of Soret number ( $Sr$ ) and falls under the effect of Schmidt number ( $Sc$ ).

**Conclusions**

This work investigated the effects of thermal diffusion on an unsteady MHD flow and heat transfer along a porous flat plate with viscous dissipation and heat absorption. The governing equations are approximated to a system of linear ordinary differential equations by using suitable similarity transformations. Numerical calculations are carried

out for various values of the dimensionless numbers of the problem using an efficient finite element method. The results are presented graphically and we can conclude that the flow field and the quantities of physical interest are significantly influenced by these numbers.

1. The velocity increases as the Grashof number, Modified Grashof number, Eckert number and Soret number increases. However, the velocity was found to decrease as the Hartmann number, Prandtl number, Schmidt number and heat absorption coefficient are increases.
2. The fluid temperature was found to increase as the Eckert number and to decrease as the Prandtl number and heat absorption coefficient are increases.
3. The concentration decreases as the Schmidt number increase and increases as the Soret effect increase.
4. The skin – friction ( $\tau$ ) due to velocity increases as the Grashof number, Modified Grashof number, Eckert number and Soret number increases. However, the velocity was found to decrease as the Hartmann number, Prandtl number, Schmidt number and heat absorption coefficient are increases.
5. Nusselt number ( $Nu$ ) due to temperature found to increase as the Eckert number and to decrease as the Prandtl number and heat absorption coefficient are increases.
6. Sherwood number ( $Sh$ ) due concentration decreases as the Schmidt number increase and increases as the Soret effect increase.

**References**

[1] Brinkman H. C, "A calculation of viscous force extended by flowing fluid in a dense swarm of particles". *Appl.Sci.Res A* (1), 27 - 34 1947.

[2] Hasimoto H, "Boundary layer growth on a flat plate with suction or injection". *J. Phys.Soc. Japan* 12, 68 - 72 1957.

[3] Berman A.S., "Laminar flow in a channel with porous wall"s, *J.Appl.Phys* 24, 1232 - 1235,1953.

[4] Sellars J.R., "Laminar flow in channels with porous walls at high suction Reynolds number", *J.Appl Phys* 26, 489 – 490, 1953.

[5] Mori Y, "on combined free and forced convective laminar MHD flow and heat transfer in channels with transverse magnetic field, *International developments in*

- Heat transfer*", ASME 124, 1031 – 1037, 1961.
- [6] Macey R.I., "Pressure flow patterns in a cylinder with reabsorbing walls, *Bull. Math. Biophys*", 25(1), 1963.
- [7] England W.G. and Emery A.F. "Thermal radiation effects on the laminar free convection boundary layer of an absorbing gas". *Journal of Heat Transfer* 91, 37 - 44 ,1969.
- [8] Soundalgekar V.M. and Thakar H.S. "Radiation effects on free convection flow past a semi infinite vertical plate". *Modeling Measurement and Control* B51, 31 – 40, 1993.
- [9] Mansutti D, Pontrelli G and Rajgopal K. R, "Steady flows of non-Newtonian fluids past a porous plate with suction or injection". *Int. J. Num. Method's fluids* 17, 927 - 941 ,1993.
- [10]Sattar M .A, "Free convection and mass transfer flow through a porous medium past an infinite vertical porous plate with time dependent temperature and concentration". *Ind. J. Pure and Appl. Math.* 23, 759 – 766, 1994.
- [11]Das U.N., Deka R.K. and Soundalgekar V.M.: "Radiation effects on flow past an impulsively started vertical infinite plate". *J.Theoretical Mechanics* 1, 111 – 115, 1996.
- [12]Chowdhary R and Das A , "Magneto-hydrodynamic boundary layer flows of non-Newtonian fluid past a flat plate". *Ind. J. Pure Appl. Math.* 31 (11), 1429– 1441, 2000.
- [13]Das S. S, Sahoo S. K and Dash G. C, "Numerical solution of mass transfer effects on unsteady flow past an accelerated vertical porous plate with suction". *Bulletin of Malysie. Math. Sci. Soc.* 29(1), 33 – 42, 2006.